Can one use Mueller Navelet jets at LHC as a clean test of QCD resummation effects at high energy?

Samuel Wallon

Université Pierre et Marie Curie

and

Laboratoire de Physique Théorique
CNRS / Université Paris Sud
Orsay

Low-x International workshop
(Low-x 2013)

June 3nd 2013

Weizmann Institute of Science, Rehovot; Hotel King Solomon, Eilat

in collaboration with

B. Ducloué (LPT Orsay) L. Szymanowski (NCBJ, Warsaw)

D. Colferai, F. Schwennsen, L. Szymanowski, S. Wallon, JHEP 12 (2010) 026 [arXiv:1002.1365]

B.D., L. Szymanowski, S. Wallon, arXiv:1208.6111

B.D., L. Szymanowski, S. Wallon, JHEP 05 (2013) 096 [arXiv:1302.7012]

Motivations

- One of the important longstanding theoretical questions raised by QCD is its behaviour in the perturbative Regge limit $s \gg -t$
- Based on theoretical grounds, one should identify and test suitable observables in order to test this peculiar dynamics

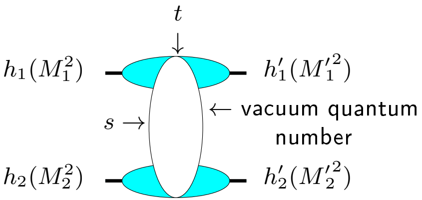

hard scales: $M_1^2,\, M_2^2 \gg \Lambda_{QCD}^2$ or $M_1'^2,\, M_2'^2 \gg \Lambda_{QCD}^2$ or $t \gg \Lambda_{QCD}^2$
where the $t-$channel exchanged state is the so-called hard Pomeron

How to test QCD in the perturbative Regge limit?

What kind of observable?

- perturbation theory should be applicable:
  selecting external or internal probes with transverse sizes $\ll 1/\Lambda_{QCD}$ (*hard* γ^*, *heavy* meson $(J/\Psi, \Upsilon)$, *energetic* forward jets) or by choosing large t in order to provide the hard scale.

- governed by the *"soft"* perturbative dynamics of QCD

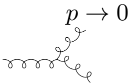

and *not* by its *collinear* dynamics

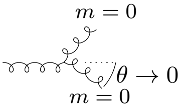

$\Longrightarrow$ select semi-hard processes with $s \gg p_{T\,i}^2 \gg \Lambda_{QCD}^2$ where $p_{T\,i}^2$ are typical transverse scale, all of the same order.

How to test QCD in the perturbative Regge limit?

Some examples of processes

- inclusive: DIS (HERA), diffractive DIS, total $\gamma^*\gamma^*$ cross-section (LEP, ILC)
- semi-inclusive: forward jet and π^0 production in DIS, Mueller-Navelet double jets, diffractive double jets, high p_T central jet, in hadron-hadron colliders (Tevatron, LHC)
- exclusive: exclusive meson production in DIS, double diffractive meson production at e^+e^- colliders (ILC), ultraperipheral events at LHC ($\mathbb{P}$omeron, $\mathbb{O}$dderon)

The specific case of QCD at large s

QCD in the perturbative Regge limit

- Small values of α_S (perturbation theory applies due to hard scales) can be compensated by large $\ln s$ enhancements. $\Rightarrow$ resummation of $\sum_n (\alpha_S \ln s)^n$ series (Balitski, Fadin, Kuraev, Lipatov)

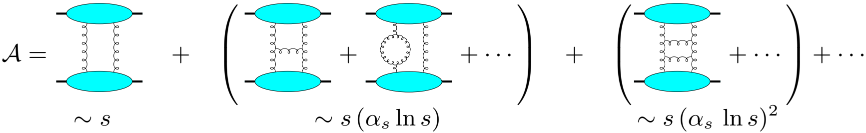

- this results in the effective BFKL ladder

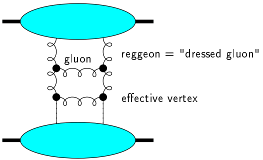

$$\Longrightarrow \sigma_{tot}^{h_1\,h_2 \to anything} = \frac{1}{s} Im\mathcal{A} \sim s^{\alpha_{\mathbb{P}}(0)-1}$$

with $\alpha_{\mathbb{P}}(0) - 1 = C\,\alpha_s \quad (C > 0)$ Leading Log Pomeron
Balitsky, Fadin, Kuraev, Lipatov

Opening the boxes: Impact representation $\gamma^* \gamma^* \to \gamma^* \gamma^*$ as an example

- Sudakov decomposition: $k_i = \alpha_i\, p_1 + \beta_i\, p_2 + k_{\perp i}$ $\quad (p_1^2 = p_2^2 = 0,\ 2p_1 \cdot p_2 = s)$
- write $\quad d^4 k_i = \frac{s}{2}\, d\alpha_i\, d\beta_i\, d^2 k_{\perp i}$ $\quad$ ($\underline{k}$ = Eucl. $\leftrightarrow$ $k_\perp$ = Mink.)
- $t-$channel gluons have non-sense polarizations at large s: $\epsilon^{up/down}_{NS} = \frac{2}{s}\, p_{2/1}$

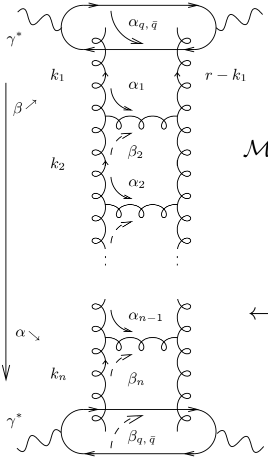

$\Rightarrow$ set $\alpha_1 = 0$ and $\int d\beta_1 \ \Rightarrow\ \Phi^{\gamma^* \to \gamma^*}(\underline{k}_1, \underline{r} - \underline{k}_1)$ impact factor

$$\mathcal{M} = \frac{is}{(2\pi)^2} \int \frac{d^2\underline{k}}{\underline{k}^2}\, \Phi^{up}(\underline{k},\, \underline{r} - \underline{k}) \int \frac{d^2\underline{k}'}{\underline{k}'^2}\, \Phi^{down}(-\underline{k}',\, -\underline{r} + \underline{k}')$$
$$\times \int_{\delta - i\infty}^{\delta + i\infty} \frac{d\omega}{2\pi i} \left(\frac{s}{s_0}\right)^{\omega} G_\omega(\underline{k}, \underline{k}', \underline{r})$$

$\longleftarrow$ multi-Regge kinematics

$\Rightarrow$ set $\beta_n = 0$ and $\int d\alpha_n \ \Rightarrow\ \Phi^{\gamma^* \to \gamma^*}(-\underline{k}_n, -\underline{r} + \underline{k}_n)$

higher order corrections

- Higher order corrections to BFKL kernel are known at NLL order (Lipatov Fadin; Camici, Ciafaloni), now for arbitrary impact parameter $\alpha_S \sum_n (\alpha_S \ln s)^n$ resummation
- impact factors are known in some cases at NLL
  - $\gamma^* \to \gamma^*$ at $t = 0$ (Bartels, Colferai, Gieseke, Kyrieleis, Qiao; Balitski, Chirilli)
  - forward jet production (Bartels, Colferai, Vacca; recently: Caporale, Ivanov, Murdaca, Papa, Perri; Chachamis, Hentschinski, Madrigal, Sabio Vera)
  - $\gamma_L^* \to \rho_L$ in the forward limit (Ivanov, Kotsky, Papa)

note: for exclusive processes, some transitions may start at twist 3

- The first computation of the $\gamma_T^* \to \rho_T$ twist 3 transition at LL has been performed only recently
  I. V. Anikin, D. Y. Ivanov, B. Pire, L. Szymanowski and S. W.
  Phys. Lett. B 688:154-167, 2010; Nucl. Phys. B 828:1-68, 2010.
- successful phenomenological application to H1 and ZEUS data for $\rho-$meson electroproduction
  I. V. Anikin, A. Besse, D. Y. Ivanov, B. Pire, L. Szymanowski and S. W.
  Phys. Rev. D 84 (2011) 054004
- first dipole model suitable for saturation effects studies at twist 3
  A. Besse, L. Szymanowski and S. W. Nucl. Phys. B 867 (2013) 16;
  arXiv :1302.1766 [hep-ph]

  see Talk by A. Besse

Mueller-Navelet jets: Basics

Mueller Navelet jets

- Consider two jets (hadron paquet within a narrow cone) separated by a large rapidity, i.e. each of them almost fly in the direction of the hadron "close" to it, and with very similar transverse momenta
- in a pure LO collinear treatment, these two jets should be emitted back to back at leading order: $\Delta\phi - \pi = 0$ ($\Delta\phi = \phi_1 - \phi_2 =$ relative azimutal angle) and $k_{\perp 1}$=$k_{\perp 2}$. There is no phase space for (untagged) emission between them

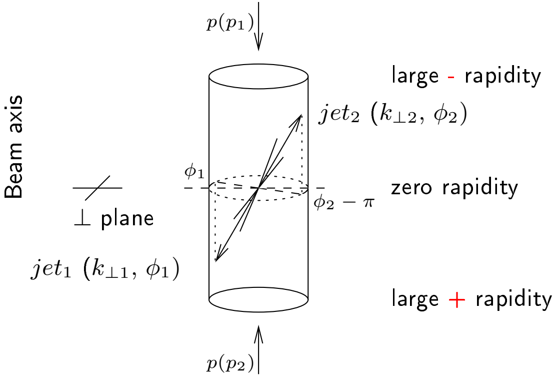

Mueller-Navelet jets at LL fails

Mueller Navelet jets at LL BFKL

- in LL BFKL ($\sim \sum(\alpha_s \ln s)^n$), emission between these jets $\longrightarrow$ strong decorrelation between the relative azimutal angle jets, incompatible with $p\bar{p}$ Tevatron collider data
- a collinear treatment at next-to-leading order (NLO) can describe the data
- important issue: non-conservation of energy-momentum along the BFKL ladder. A LL BFKL-based Monte Carlo combined with e-m conservation improves dramatically the situation (Orr and Stirling)

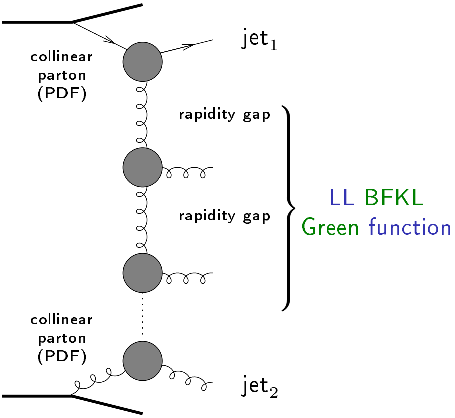

Multi-Regge kinematics (LL BFKL)

Studies at LHC: Mueller-Navelet jets

Mueller Navelet jets at NLL BFKL

- up to now, the subseries $\alpha_s \sum (\alpha_s \ln s)^n$ NLL was included only in the exchanged $\mathbb{P}$omeron state, and not inside the jet vertices Sabio Vera, Schwennsen Marquet, Royon
- the common belief was that these corrections should not be important

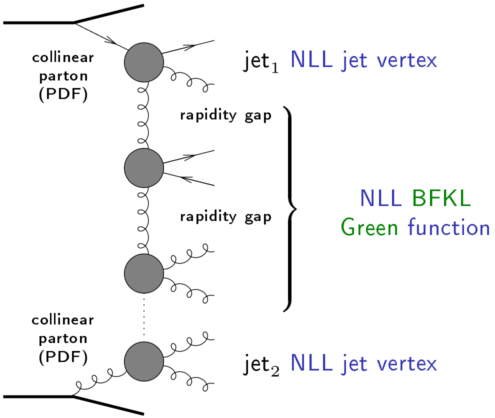

Quasi Multi-Regge kinematics (here for NLL BFKL)

Master formulas

k_T-factorized differential cross-section

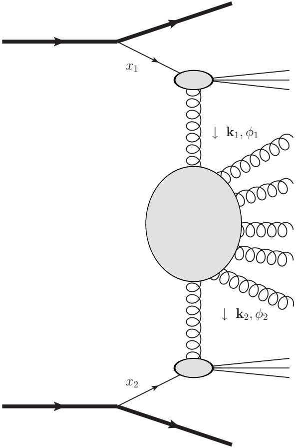

$$\frac{d\sigma}{d|\mathbf{k}_{J,1}|\, d|\mathbf{k}_{J,2}|\, dy_{J,1}\, dy_{J,2}} = \int d\phi_{J,1}\, d\phi_{J,2} \int d^2\mathbf{k}_1\, d^2\mathbf{k}_2$$

$$\times\, \Phi(\mathbf{k}_{J,1}, x_{J,1}, -\mathbf{k}_1)$$

$$\times\, G(\mathbf{k}_1, \mathbf{k}_2, \hat{s})$$

$$\times\, \Phi(\mathbf{k}_{J,2}, x_{J,2}, \mathbf{k}_2)$$

with $\Phi(\mathbf{k}_{J,2}, x_{J,2}, \mathbf{k}_2) = \int dx_2\, f(x_2) V(\mathbf{k}_2, x_2)$ $\quad f \equiv$ PDF $\quad x_J = \frac{|\mathbf{k}_J|}{\sqrt{s}} e^{y_J}$

Master formulas

Angular coefficients

$$\mathcal{C}_m \equiv \int d\phi_{J,1}\, d\phi_{J,2}\, \cos\left(m(\phi_{J,1} - \phi_{J,2} - \pi)\right)$$

$$\times \int d^2\mathbf{k}_1\, d^2\mathbf{k}_2\, \Phi(\mathbf{k}_{J,1}, x_{J,1}, -\mathbf{k}_1)\, G(\mathbf{k}_1, \mathbf{k}_2, \hat{s})\, \Phi(\mathbf{k}_{J,2}, x_{J,2}, \mathbf{k}_2).$$

- $m = 0 \implies$ cross-section

$$\frac{d\sigma}{d|\mathbf{k}_{J,1}|\, d|\mathbf{k}_{J,2}|\, dy_{J,1}\, dy_{J,2}} = \mathcal{C}_0$$

- $m > 0 \implies$ azimutal decorrelation

$$\langle \cos(m\varphi) \rangle \equiv \langle \cos\left(m(\phi_{J,1} - \phi_{J,2} - \pi)\right) \rangle = \frac{\mathcal{C}_m}{\mathcal{C}_0}$$

Master formulas in conformal variables

Rely on LL BFKL eigenfunctions

- LL BFKL eigenfunctions: $E_{n,\nu}(\mathbf{k}_1) = \frac{1}{\pi\sqrt{2}} \left(\mathbf{k}_1^2\right)^{i\nu-\frac{1}{2}} e^{in\phi_1}$
- decompose Φ on this basis
- use the known LL eigenvalue of the BFKL equation on this basis:

$$\omega(n,\nu) = \bar{\alpha}_s \chi_0\left(|n|, \tfrac{1}{2}+i\nu\right)$$

with $\chi_0(n,\gamma) = 2\Psi(1) - \Psi\left(\gamma+\frac{n}{2}\right) - \Psi\left(1-\gamma+\frac{n}{2}\right)$

$(\Psi(x) = \Gamma'(x)/\Gamma(x),\ \bar{\alpha}_s = N_c\alpha_s/\pi)$

- $\Longrightarrow$ master formula:

$$\mathcal{C}_m = (4-3\,\delta_{m,0}) \int \mathrm{d}\nu\, C_{m,\nu}(|\mathbf{k}_{J,1}|, x_{J,1})\, C^*_{m,\nu}(|\mathbf{k}_{J,2}|, x_{J,2}) \left(\frac{\hat{s}}{s_0}\right)^{\omega(m,\nu)}$$

with $\quad C_{m,\nu}(|\mathbf{k}_J|, x_J) = \int \mathrm{d}\phi_J\, \mathrm{d}^2\mathbf{k}\, \mathrm{d}x\, f(x) V(\mathbf{k},x) E_{m,\nu}(\mathbf{k}) \cos(m\phi_J)$

- at NLL, same master formula: just change $\omega(m,\nu)$ and V (although $E_{n,\nu}$ are not anymore eigenfunctions)
- one may improve the NLL BFKL kernel by imposing its compatibility with DGLAP in the (anti)collinear limit (poles in $\gamma = 1/2 + i\nu$ plane) Salam; Ciafaloni, Colferai
note: NLL vertices are free of γ poles

Numerical implementation

In practice: two codes have been developed

A *Mathematica* code, exploratory

D. Colferai, F. Schwennsen, L. Szymanowski, S. W.
JHEP 1012:026 (2010) 1-72 [arXiv:1002.1365 [hep-ph]]

- jet cone-algorithm with $R = 0.5$
- MSTW 2008 PDFs (available as *Mathematica* packages)
- $\mu_R = \mu_F$ (in MSTW 2008 PDFs); we take $\mu_R = \mu_F = \sqrt{|\mathbf{k}_{J,1}|\,|\mathbf{k}_{J,2}|}$
- two-loop running coupling $\alpha_s(\mu_R^2)$
- we use a ν grid (with a dense sampling around 0)
- we use Cuba integration routines (in practice Vegas): precision 10^{-2} for 500.000 max points per integration
- mapping $|\mathbf{k}| = |\mathbf{k}_J| \tan(\xi\pi/2)$ for $\mathbf{k}$ integrations $\Rightarrow [0, \infty[\to [0, 1]$
- although formally the results should be finite, it requires a special grouping of the integrand in order to get stable results
  $\Longrightarrow$ 14 minimal stable basic blocks to be evaluated numerically
- rather slow code

Numerical implementation

A *Fortran* code, $\simeq 20$ times faster

B. Ducloué, L. Szymanowski, S.W.
JHEP 05 (2013) 096 [arXiv:1207.7012 [hep-ph]]

- Check of our *Mathematica* based results
- Detailled check of previous mixed studies (NLL Green's function + LL jet vertices)
- Allows for k_J integration in a finite range
- Stability studies (PDFs, etc...) made easier
- Comparison with the recent small R study of D. Yu. Ivanov, A. Papa
- Azimuthal distribution
- More detailled comparison with fixed order NLO: NEW CONCLUSIONS
- Problems remain with ν integration for low Y
  (for $Y < \frac{\pi}{2\alpha_s N_c} \sim 4$). To be fixed!

  We restrict ourselves to $Y > 4$.

Integration over $|\mathbf{k}_J|$

Experimental data is integrated over some range, $k_{J\text{min}} \leq k_J = |\mathbf{k}_J|$

Growth of the cross section with increasing $k_{J\text{max}}$:

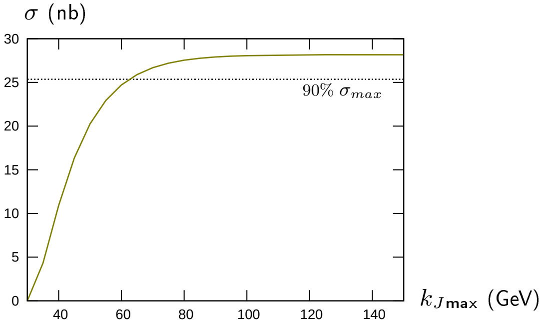

$\Rightarrow$ need to integrate up to $k_{J\text{max}} \sim 60$ GeV

A consistency check of stability of $|\mathbf{k}_J|$ integration have been made:

- consider the simplified NLL Green's function + LL jet vertices scenario
- the integration $\int_{k_{J\,min}}^{\infty} dk_J$ can be performed analytically
- comparison with integrated results of Sabio Vera, Schwennsen is safe

Integration over $|\mathbf{k}_J|$

Energy-momentum conservation issues

- BFKL does not preserve energy-momentum conservation
- This violation is expected to be smaller at higher order in perturbation theory, i.e. NLL versus LL
- In practice: avoid to use all the available collider energy: $Y_{J,i} \ll \cosh^{-1} \frac{x_i\, E}{k_{J,i}}$
  $\rightarrow$ A lower k_J means a larger validity domain : a k_J as small as possible is preferable
- With only a lower cut on k_J, one has to integrate over regions where the BFKL approach may not be valid anymore : $k_J = 60$ GeV $\rightarrow Y_{J,i} \ll 3.7$
- For this reason it would be nice to have a measurement with also an upper cut on transverse momentum, $k_{J\text{min}} \leq k_J \leq k_{J\text{max}}$
  note: large cross-sections $\Rightarrow$ narrow bining in k_J is only a detector issue
- CMS: $k_{J\text{min}} = 35$ GeV
  Going down to 20 GeV would probably require a dedicated trigger
- note that:
  - k_J integration reduces the Y domain between jets
  - x_i integration weighted by PDFs reduces the Y domain between jets

Checks: fixed R versus small R limit

Comparison between the exact R and approximated small R treatments

e.g. : $|\mathbf{k}_{J,1}| = 30\,\mathrm{GeV}$, $|\mathbf{k}_{J,2}| = 35\,\mathrm{GeV}$ $\sqrt{s} = 7$ TeV

$\frac{\sigma_{\text{exact}} - \sigma_{\text{approx.}}}{\sigma_{\text{exact}}}$ $R = .3$

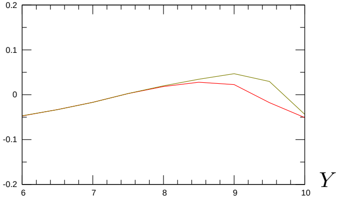

$\frac{\sigma_{\text{exact}} - \sigma_{\text{approx.}}}{\sigma_{\text{exact}}}$ $R = .5$

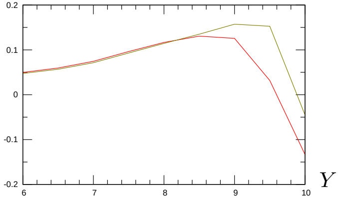

$\frac{\langle \cos\varphi\rangle_{\text{exact}} - \langle \cos\varphi\rangle_{\text{approx.}}}{\langle \cos\varphi\rangle_{\text{exact}}}$ $R = .3$

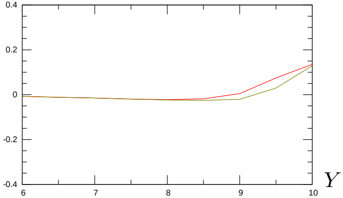

$\frac{\langle \cos\varphi\rangle_{\text{exact}} - \langle \cos\varphi\rangle_{\text{approx.}}}{\langle \cos\varphi\rangle_{\text{exact}}}$ $R = .5$

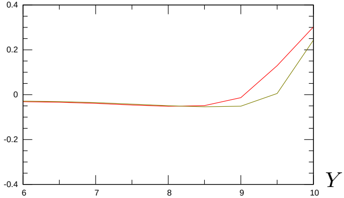

small R approximation: see D. Yu. Ivanov, A. Papa

Results: symmetric configuration ($|\mathbf{k}_{J,1\,\min}| = |\mathbf{k}_{J,2\,\min}| = 35\,\text{GeV}$) $\sqrt{s} = 7$ TeV

Cross-section

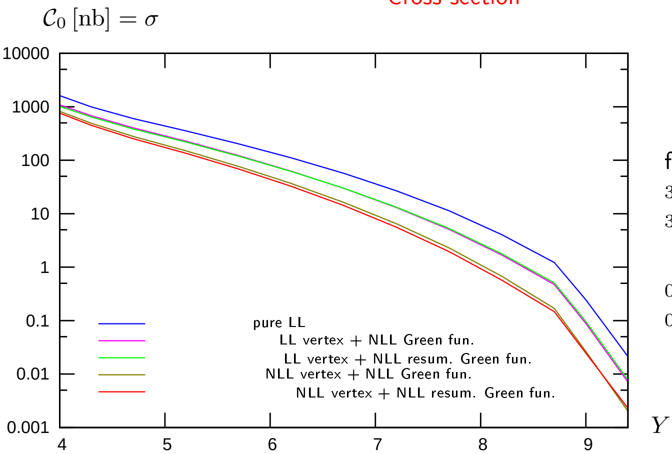

for typical CMS bins:

$35\,\text{GeV} < |\mathbf{k}_{J,1}| < 60\,\text{GeV}$

$35\,\text{GeV} < |\mathbf{k}_{J,2}| < 60\,\text{GeV}$

$0 < Y_1 < 4.7$

$0 < Y_2 < 4.7$

- error bands = errors due to the Monte Carlo integration (2% to 5%)
- NLL vertex correction very sizeable $\sim$ NLL Green's function effects
- Energy-momentum conservation not satisfied by BFKL-like approaches $\Rightarrow$ validity restricted to $Y_{J,i} \ll \cosh^{-1} \frac{x_i\,E}{k_{J,i}}$: $Y = Y_1 + Y_2 \ll 8.4$ for $x \sim 1/3$

Results: symmetric configuration $(|\mathbf{k}_{J,1\,\min}| = |\mathbf{k}_{J,2\,\min}| = 35\,\text{GeV})$ $\sqrt{s} = 7$ TeV

Cross-section: stability with respect to s_0 and $\mu_R = \mu_F$ changes

(full NLL approach)

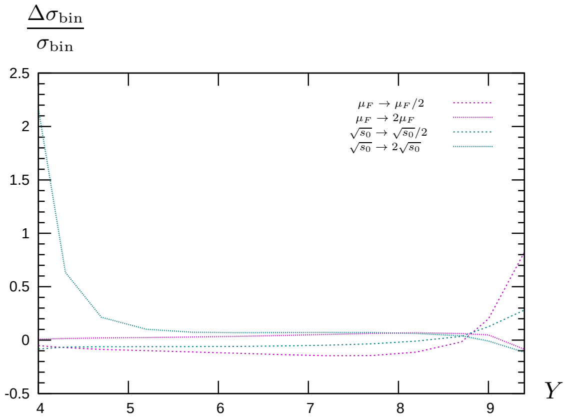

$35\,\text{GeV} < |\mathbf{k}_{J,1}| < 60\,\text{GeV}$

$35\,\text{GeV} < |\mathbf{k}_{J,2}| < 60\,\text{GeV}$

$0 < Y_1 < 4.7$

$0 < Y_2 < 4.7$

Results: symmetric configuration $(|\mathbf{k}_{J,1\ \mathrm{min}}| = |\mathbf{k}_{J,2\ \mathrm{min}}| = 35\,\mathrm{GeV})$ $\sqrt{s} = 7$ TeV

Cross-section: PDF errors

Relative variation of the cross section: other PDF sets versus MSTW 2008

(full NLL approach)

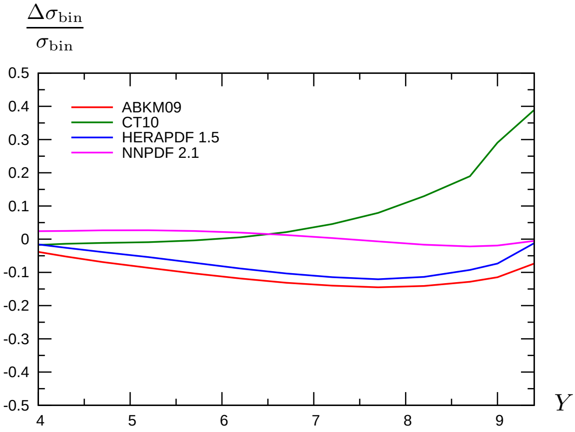

$35\,\mathrm{GeV} < |\mathbf{k}_{J,1}| < 60\,\mathrm{GeV}$
$35\,\mathrm{GeV} < |\mathbf{k}_{J,2}| < 60\,\mathrm{GeV}$

$0 < Y_1 < 4.7$
$0 < Y_2 < 4.7$

(very similar values for the LL computation)

Results: symmetric configuration $(|\mathbf{k}_{J,1\,\min}| = |\mathbf{k}_{J,2\,\min}| = 35\,\mathrm{GeV})$ $\sqrt{s} = 7$ TeV

Azimuthal correlation $\langle \cos\varphi \rangle$

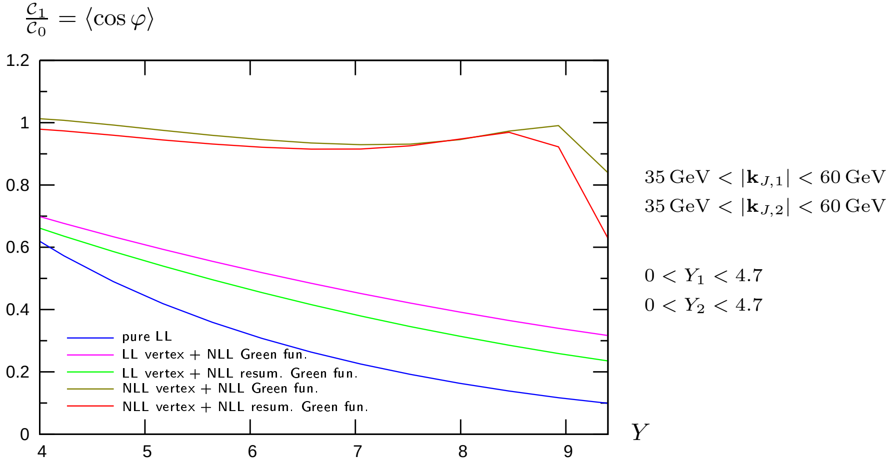

- LL $\rightarrow$ NLL vertices change results dramatically: $\langle \cos\varphi \rangle$ now flat and large
- The (anti)collinear resummation effects are not very sizable at full NLL this is a good sign of stability of this full NLL-BFKL treatment

Results: symmetric configuration ($|\mathbf{k}_{J,1\ \mathrm{min}}| = |\mathbf{k}_{J,2\ \mathrm{min}}| = 35\,\mathrm{GeV}$) $\sqrt{s} = 7$ TeV

Azimuthal correlation $\langle \cos\varphi \rangle$:
more on the (anti)collinear resummation effects

$|\mathbf{k}_{J,1}| = |\mathbf{k}_{J,2}| = 35\,\mathrm{GeV}$ $\quad 0 < Y_1, Y_2 < 4.7$

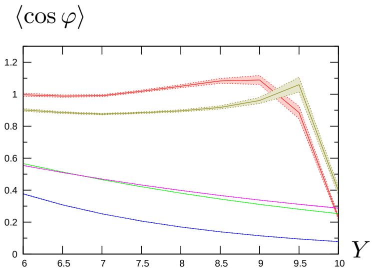

pure LL
LL vertices + NLL Green's fun.
LL vertices + NLL resum. $(n = 0)$ Green's fun.
NLL vertices + NLL Green's fun.
NLL vertices + NLL resum. $(n = 0)$ Green's fun.

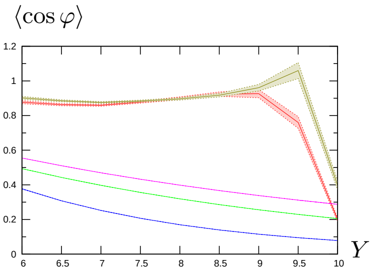

pure LL
LL vertices + NLL Green's fun.
LL vertices + NLL resum. (all n) Green's fun.
NLL vertices + NLL Green's fun.
NLL vertices + NLL resum. (all n) Green's fun.

Results: symmetric configuration $(|\mathbf{k}_{J,1\ \min}| = |\mathbf{k}_{J,2\ \min}| = 35\,\mathrm{GeV})$ $\sqrt{s} = 7$ TeV

Azimuthal correlation $\langle\cos\varphi\rangle$: PDF errors

Relative variation of $\langle\cos\varphi\rangle$: other PDF sets versus MSTW 2008

(full NLL approach)

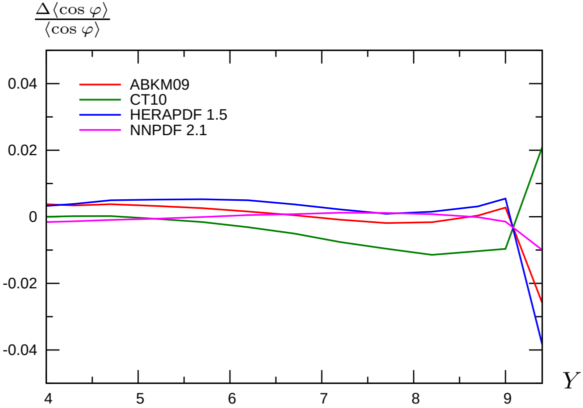

$35\,\mathrm{GeV} < |\mathbf{k}_{J,1}| < 60\,\mathrm{GeV}$

$35\,\mathrm{GeV} < |\mathbf{k}_{J,2}| < 60\,\mathrm{GeV}$

$0 < Y_1 < 4.7$

$0 < Y_2 < 4.7$

$\langle\cos\varphi\rangle$ is much less sensitive to the PDFs than the cross section (at LL $\langle\cos\varphi\rangle$ does not depend on the PDFs at all)

Results: symmetric configuration ($|\mathbf{k}_{J,1\,\min}| = |\mathbf{k}_{J,2\,\min}| = 35\,\mathrm{GeV}$) $\sqrt{s} = 7$ TeV

Azimuthal correlation $\langle \cos\varphi \rangle$:

stability with respect to s_0 and $\mu_R = \mu_F$

(full NLL approach)

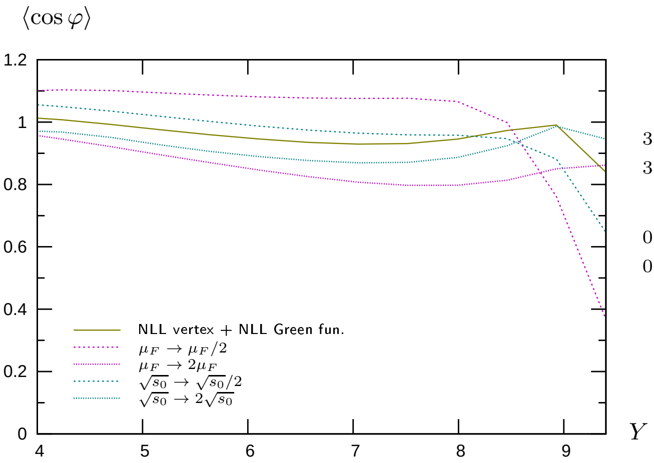

$35\,\mathrm{GeV} < |\mathbf{k}_{J,1}| < 60\,\mathrm{GeV}$

$35\,\mathrm{GeV} < |\mathbf{k}_{J,2}| < 60\,\mathrm{GeV}$

$0 < Y_1 < 4.7$

$0 < Y_2 < 4.7$

Results: symmetric configuration ($|\mathbf{k}_{J,1\ \min}| = |\mathbf{k}_{J,2\ \min}| = 35\,\text{GeV}$) $\sqrt{s} = 7$ TeV

Azimuthal correlation $\langle \cos\varphi \rangle$:

comparison of our full NLL prediction with CMS data

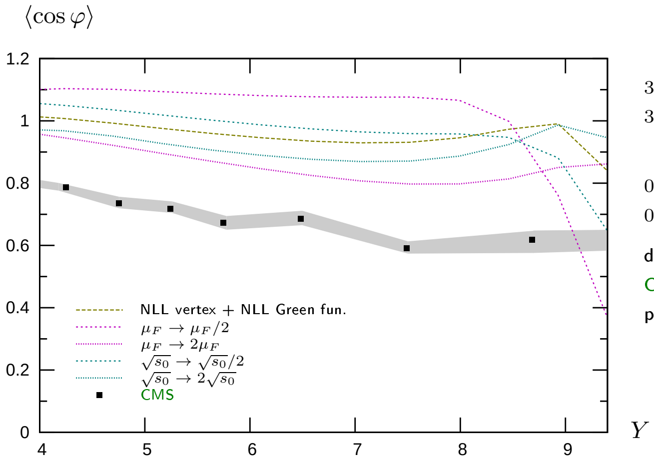

$35\,\text{GeV} < |\mathbf{k}_{J,1}| < 60\,\text{GeV}$
$35\,\text{GeV} < |\mathbf{k}_{J,2}| < 60\,\text{GeV}$

$0 < Y_1 < 4.7$
$0 < Y_2 < 4.7$

data from CMS-PAS-FSQ-12-002, presented at DIS 2013

Results: symmetric configuration ($|\mathbf{k}_{J,1\ \min}| = |\mathbf{k}_{J,2\ \min}| = 35\ \text{GeV}$) $\sqrt{s} = 7$ TeV

Azimuthal correlation $\langle \cos 2\varphi \rangle$

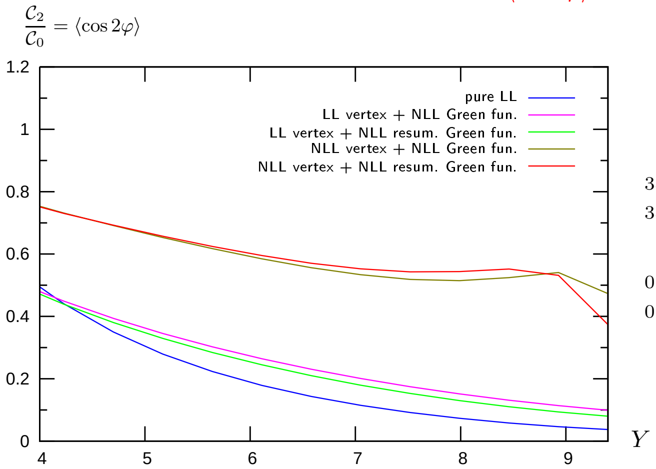

$35\ \text{GeV} < |\mathbf{k}_{J,1}| < 60\ \text{GeV}$
$35\ \text{GeV} < |\mathbf{k}_{J,2}| < 60\ \text{GeV}$

$0 < Y_1 < 4.7$
$0 < Y_2 < 4.7$

- LL $\rightarrow$ NLL vertices change results dramatically
- The (anti)collinear resummation effects are not very sizable at full NLL this is a good sign of stability of this full NLL-BFKL treatment

Results: symmetric configuration ($|\mathbf{k}_{J,1\ \min}| = |\mathbf{k}_{J,2\ \min}| = 35\,\mathrm{GeV}$) $\sqrt{s} = 7$ TeV

Azimuthal correlation $\langle \cos 2\varphi \rangle$:

stability with respect to s_0 and $\mu_R = \mu_F$

(full NLL approach)

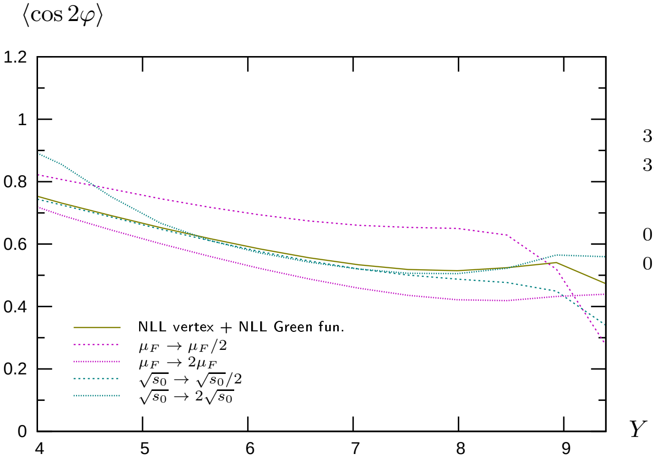

$35\,\mathrm{GeV} < |\mathbf{k}_{J,1}| < 60\,\mathrm{GeV}$
$35\,\mathrm{GeV} < |\mathbf{k}_{J,2}| < 60\,\mathrm{GeV}$

$0 < Y_1 < 4.7$
$0 < Y_2 < 4.7$

Results: symmetric configuration ($|\mathbf{k}_{J,1\,\min}| = |\mathbf{k}_{J,2\,\min}| = 35\,\mathrm{GeV}$) $\sqrt{s} = 7$ TeV

Azimuthal correlation $\langle \cos 2\varphi \rangle$:

comparison of our full NLL prediction with CMS data

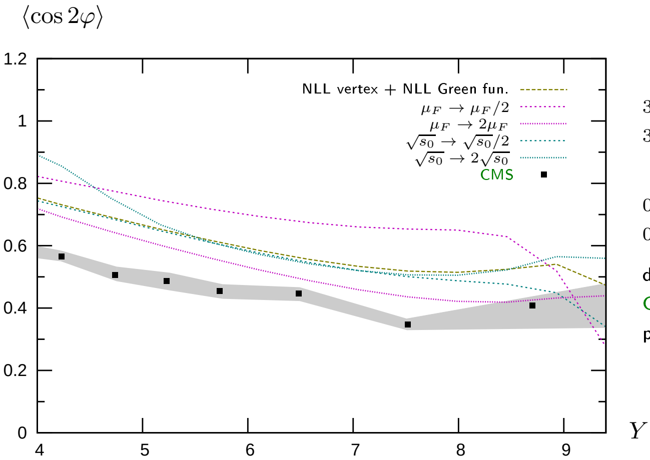

$35\,\mathrm{GeV} < |\mathbf{k}_{J,1}| < 60\,\mathrm{GeV}$

$35\,\mathrm{GeV} < |\mathbf{k}_{J,2}| < 60\,\mathrm{GeV}$

$0 < Y_1 < 4.7$

$0 < Y_2 < 4.7$

data from CMS-PAS-FSQ-12-002, presented at DIS 2013

Results: symmetric configuration ($|\mathbf{k}_{J,1\ \min}| = |\mathbf{k}_{J,2\ \min}| = 35\,\mathrm{GeV}$) $\sqrt{s} = 7$ TeV

Azimuthal correlation $\langle \cos 2\varphi \rangle / \langle \cos \varphi \rangle$

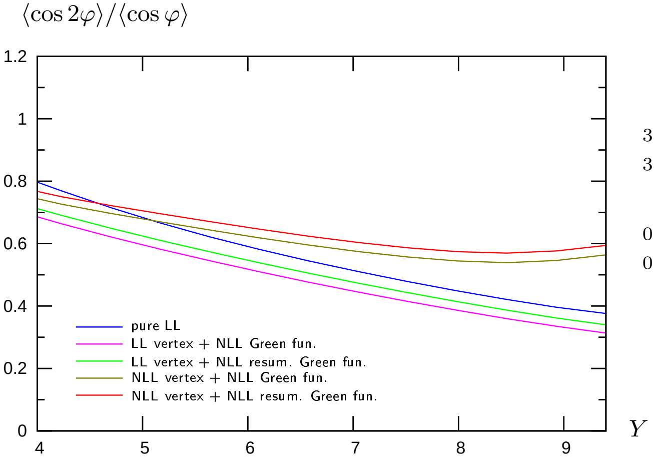

$35\,\mathrm{GeV} < |\mathbf{k}_{J,1}| < 60\,\mathrm{GeV}$

$35\,\mathrm{GeV} < |\mathbf{k}_{J,2}| < 60\,\mathrm{GeV}$

$0 < Y_1 < 4.7$

$0 < Y_2 < 4.7$

Results: symmetric configuration ($|\mathbf{k}_{J,1\ \min}| = |\mathbf{k}_{J,2\ \min}| = 35\ \mathrm{GeV}$) $\sqrt{s} = 7$ TeV

Azimuthal correlation: PDF errors

Relative variation of $\frac{\langle \cos 2\varphi \rangle}{\langle \cos \varphi \rangle}$: other PDF sets versus MSTW 2008

(full NLL approach)

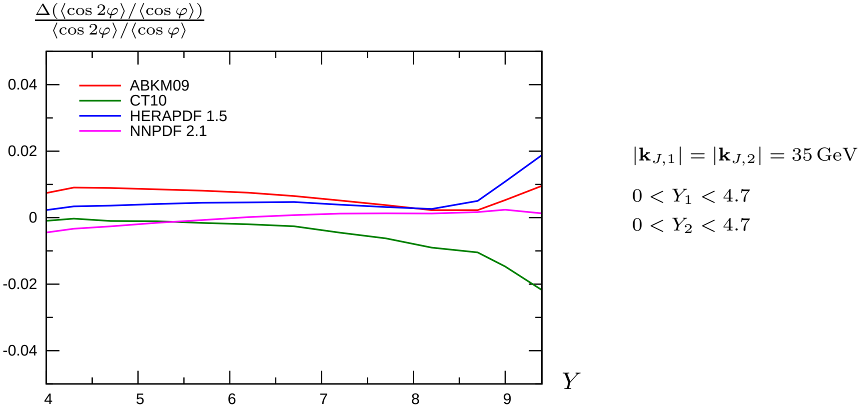

$\langle \cos 2\varphi \rangle / \langle \cos \varphi \rangle$ is much less sensitive to the PDFs than the cross section

Results: symmetric configuration $(|\mathbf{k}_{J,1\ \mathrm{min}}| = |\mathbf{k}_{J,2\ \mathrm{min}}| = 35\,\mathrm{GeV})$ $\sqrt{s} = 7$ TeV

Azimuthal correlation $\langle\cos 2\varphi\rangle/\langle\cos\varphi\rangle$:

stability with respect to s_0 and $\mu_R = \mu_F$

(full NLL approach)

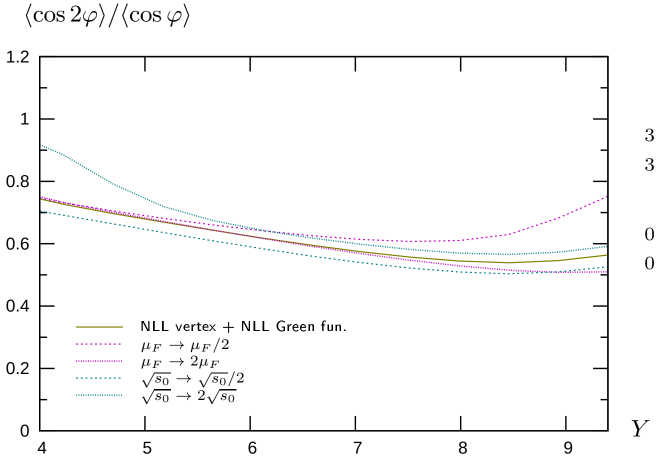

$35\,\mathrm{GeV} < |\mathbf{k}_{J,1}| < 60\,\mathrm{GeV}$
$35\,\mathrm{GeV} < |\mathbf{k}_{J,2}| < 60\,\mathrm{GeV}$

$0 < Y_1 < 4.7$
$0 < Y_2 < 4.7$

Very good stability in the range $5 < Y < 8$

Results: symmetric configuration $(|\mathbf{k}_{J,1\,\min}| = |\mathbf{k}_{J,2\,\min}| = 35\,\mathrm{GeV})$ $\sqrt{s} = 7$ TeV

Azimuthal correlation $\langle\cos 2\varphi\rangle/\langle\cos\varphi\rangle$:

comparison of our full NLL prediction with CMS data

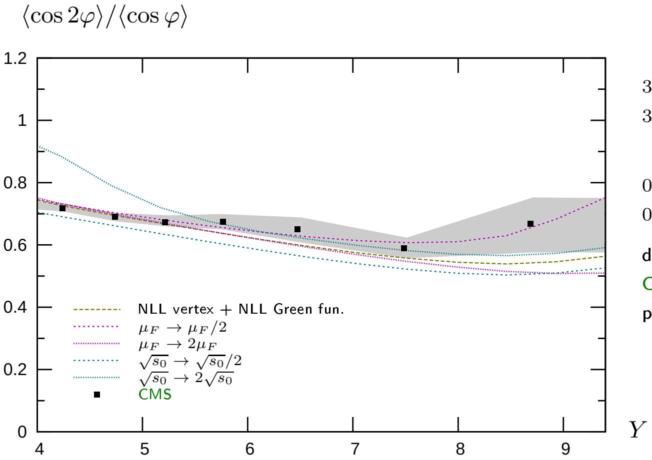

$35\,\mathrm{GeV} < |\mathbf{k}_{J,1}| < 60\,\mathrm{GeV}$

$35\,\mathrm{GeV} < |\mathbf{k}_{J,2}| < 60\,\mathrm{GeV}$

$0 < Y_1 < 4.7$

$0 < Y_2 < 4.7$

data from CMS-PAS-FSQ-12-002, presented at DIS 2013

Very good stability in the range $5 < Y < 8$

Results: symmetric configuration $(|\mathbf{k}_{J,1\ \mathrm{min}}| = |\mathbf{k}_{J,2\ \mathrm{min}}| = 35\ \mathrm{GeV})$ $\sqrt{s} = 7$ TeV

Azimuthal correlation $\langle \cos 3\varphi \rangle$ and $\langle \cos 3\varphi \rangle / \langle \cos 2\varphi \rangle$:
predictions and comparison with CMS data

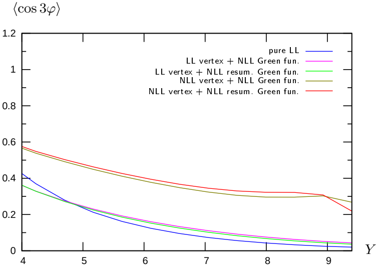

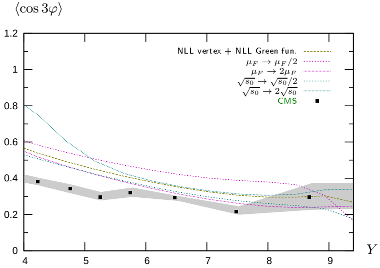

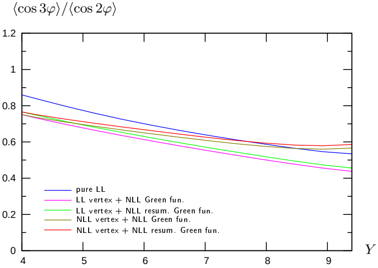

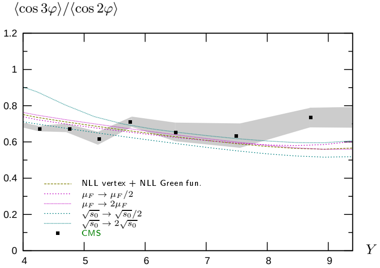

Results: symmetric configuration $(|\mathbf{k}_{J,1\ \mathrm{min}}| = |\mathbf{k}_{J,2\ \mathrm{min}}| = 35\,\mathrm{GeV})$ $\sqrt{s} = 7$ TeV

Azimuthal distribution

Computing $\langle \cos(n\phi) \rangle$ up to large values of n gives access to the angular distribution

$$\frac{1}{\sigma}\frac{d\sigma}{d\phi} = \frac{1}{2\pi}\left\{1 + 2\sum_{n=1}^{\infty}\cos(n\phi)\,\langle\cos(n\phi)\rangle\right\}$$

This is a quantity accessible at experiments like ATLAS and CMS

Results: symmetric configuration $(|\mathbf{k}_{J,1\,\min}| = |\mathbf{k}_{J,2\,\min}| = 35\,\mathrm{GeV})$ $\sqrt{s} = 7$ TeV

Azimuthal distribution

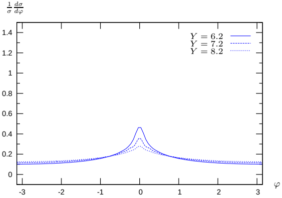

pure LL

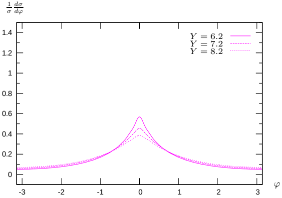

LL vertices + NLL Green's fun.

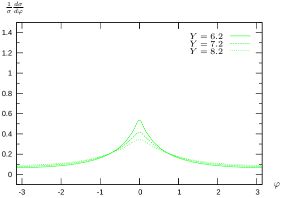

LL vert. + NLL resum. Green's fun.

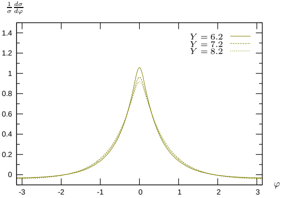

NLL vert. + NLL Green's fun.

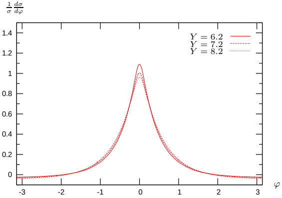

NLL vert. + NLL resum. Green's fun.

$35\,\mathrm{GeV} < |\mathbf{k}_{J,1}| < 60\,\mathrm{GeV}$
$35\,\mathrm{GeV} < |\mathbf{k}_{J,2}| < 60\,\mathrm{GeV}$

$0 < Y_1 < 4.7$
$0 < Y_2 < 4.7$

Full NLL treatment predicts :

- Less decorrelation for the same Y
- Slower decorrelation with increasing Y

Results: symmetric configuration ($|\mathbf{k}_{J,1\,\mathrm{min}}| = |\mathbf{k}_{J,2\,\mathrm{min}}| = 35\,\mathrm{GeV}$) $\sqrt{s} = 7$ TeV

Azimuthal distribution: stability with respect to s_0 and $\mu_R = \mu_F$

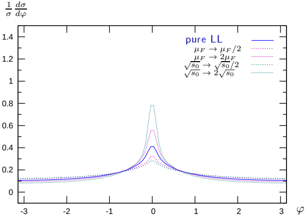

pure LL

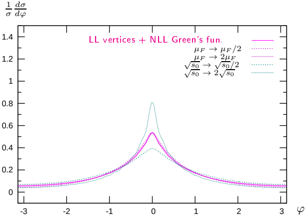

LL vertices + NLL Green's fun.

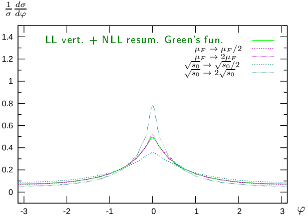

LL vert. + NLL resum. Green's fun.

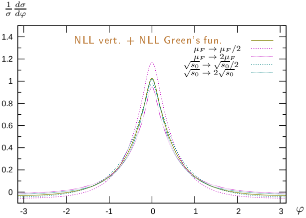

NLL vert. + NLL Green's fun.

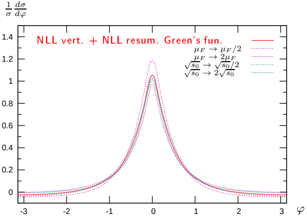

NLL vert. + NLL resum. Green's fun.

$35\,\mathrm{GeV} < |\mathbf{k}_{J,1}| < 60\,\mathrm{GeV}$

$35\,\mathrm{GeV} < |\mathbf{k}_{J,2}| < 60\,\mathrm{GeV}$

$0 < Y_1 < 4.7$

$0 < Y_2 < 4.7$

integrating on the bin:

$6 < Y = Y_1 + Y_2 < 9.4$

The predicted φ distribution within full NLL treatment is stable

Results: asymmetric configuration ($|\mathbf{k}_{J,1\,\min}| = 35\,\mathrm{GeV}$, $|\mathbf{k}_{J,2\,\min}| = 50\,\mathrm{GeV}$) $\sqrt{s} = 7$ TeV

Cross-section: fixed order NLO versus BFKL

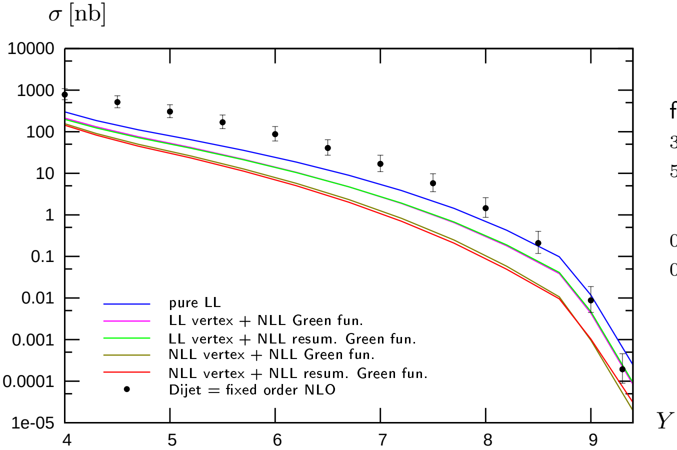

for typical CMS bins:

$35\,\mathrm{GeV} < |\mathbf{k}_{J,1}| < 60\,\mathrm{GeV}$

$50\,\mathrm{GeV} < |\mathbf{k}_{J,2}| < 60\,\mathrm{GeV}$

$0 < Y_1 < 4.7$

$0 < Y_2 < 4.7$

Such an asymmetric configuration is *required by fixed order approaches*, which are unstable for symmetric configurations.

dots = based on the fixed order NLO parton generator *Dijet* (thanks to M. Fontannaz)

Results: asymmetric config. $(|\mathbf{k}_{J,1\ \min}| = 35\,\mathrm{GeV}\,, |\mathbf{k}_{J,2\ \min}| = 50\,\mathrm{GeV})$ $\sqrt{s} = 7$ TeV

Cross-section: fixed order NLO versus BFKL NLL

Including uncertainties

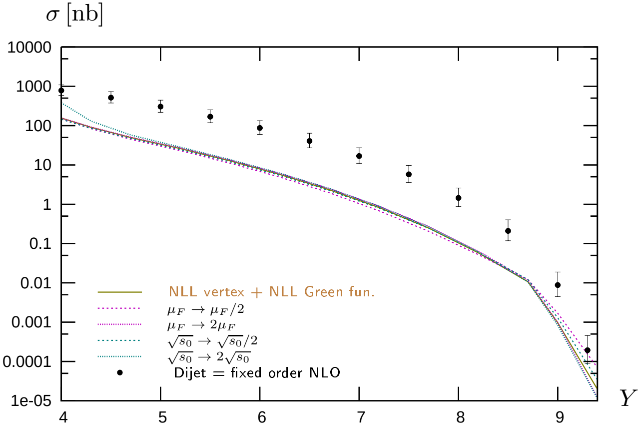

for typical CMS bins:

$35\,\mathrm{GeV} < |\mathbf{k}_{J,1}| < 60\,\mathrm{GeV}$

$50\,\mathrm{GeV} < |\mathbf{k}_{J,2}| < 60\,\mathrm{GeV}$

$0 < Y_1 < 4.7$

$0 < Y_2 < 4.7$

- Putting (almost) the same scale, exactly the same cuts, we get a noticeable difference between fixed order NLO and NLL BFKL for $4.5 < Y < 8.5$: $\sigma_{\mathrm{NLO}} > \sigma_{\mathrm{NLL\,BFKL}}$
- This result is rather stable w.r.t s_0 and μ choices.

Results: asymmetric config. $(|\mathbf{k}_{J,1\ \min}| = 35\,\text{GeV}\,, |\mathbf{k}_{J,2\ \min}| = 50\,\text{GeV})$ $\sqrt{s} = 7$ TeV

Azimuthal correlation $\langle \cos\varphi \rangle$: fixed order NLO versus BFKL

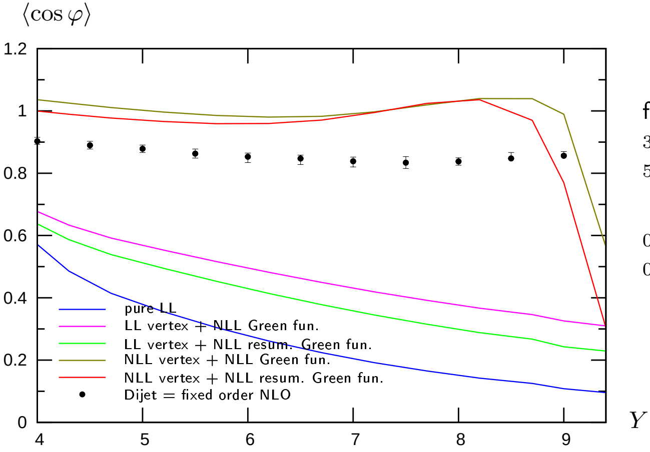

for typical CMS bins:

$35\,\text{GeV} < |\mathbf{k}_{J,1}| < 60\,\text{GeV}$

$50\,\text{GeV} < |\mathbf{k}_{J,2}| < 60\,\text{GeV}$

$0 < Y_1 < 4.7$

$0 < Y_2 < 4.7$

dots = based on the fixed order NLO parton generator *Dijet* (thanks to M. Fontannaz)

Results: asymmetric config. $(|\mathbf{k}_{J,1\ \min}| = 35\,\mathrm{GeV}\,, |\mathbf{k}_{J,2\ \min}| = 50\,\mathrm{GeV})$ $\sqrt{s} = 7$ TeV

Azimuthal correlation $\langle \cos\varphi \rangle$: fixed order NLO versus NLL BFKL

Including uncertainties

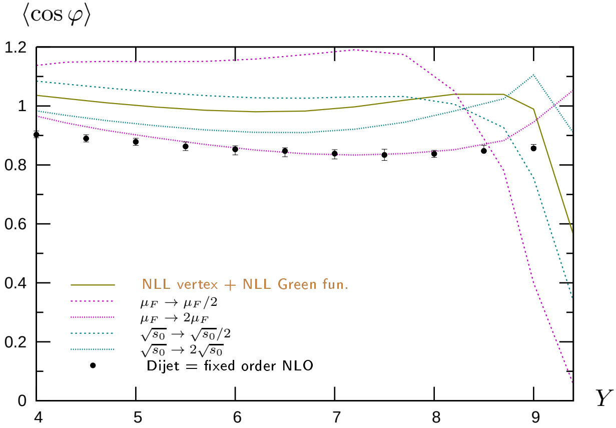

for typical CMS bins:

$35\,\mathrm{GeV} < |\mathbf{k}_{J,1}| < 60\,\mathrm{GeV}$

$50\,\mathrm{GeV} < |\mathbf{k}_{J,2}| < 60\,\mathrm{GeV}$

$0 < Y_1 < 4.7$

$0 < Y_2 < 4.7$

- Putting (almost) the same scale, exactly the same cuts, we get a difference between fixed order NLO and NLL BFKL for $4.5 < Y < 8.5$
- This difference is washed-out because of s_0 and μ dependency: $\langle \cos\varphi \rangle_{\mathrm{NLO}} \sim \langle \cos\varphi \rangle_{\mathrm{NLL\,BFKL}}$

Results: asymmetric config. ($|\mathbf{k}_{J,1\,\min}| = 35\,\mathrm{GeV}$, $|\mathbf{k}_{J,2\,\min}| = 50\,\mathrm{GeV}$) $\sqrt{s} = 7$ TeV

Azimuthal correlation $\langle \cos 2\varphi \rangle$: fixed order NLO versus BFKL

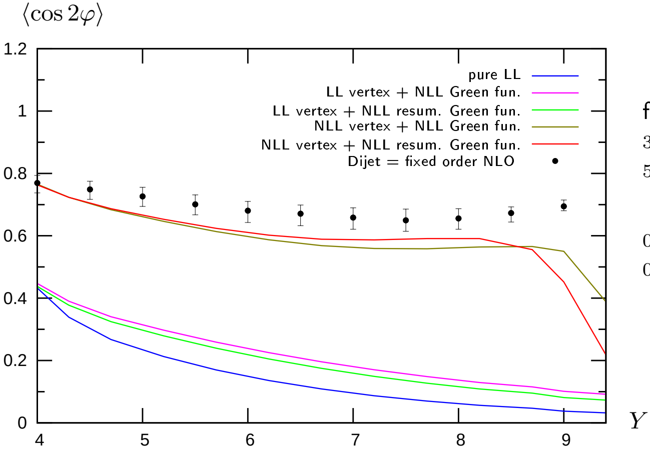

for typical CMS bins:

$35\,\mathrm{GeV} < |\mathbf{k}_{J,1}| < 60\,\mathrm{GeV}$

$50\,\mathrm{GeV} < |\mathbf{k}_{J,2}| < 60\,\mathrm{GeV}$

$0 < Y_1 < 4.7$

$0 < Y_2 < 4.7$

dots = based on the fixed order NLO parton generator *Dijet* (thanks to M. Fontannaz)

Results: asymmetric config. $(|\mathbf{k}_{J,1\ \min}| = 35\,\mathrm{GeV}\,, |\mathbf{k}_{J,2\ \min}| = 50\,\mathrm{GeV})$ $\sqrt{s} = 7$ TeV

Azimuthal correlation $\langle \cos 2\varphi \rangle$: fixed order NLO versus NLL BFKL

Including uncertainties

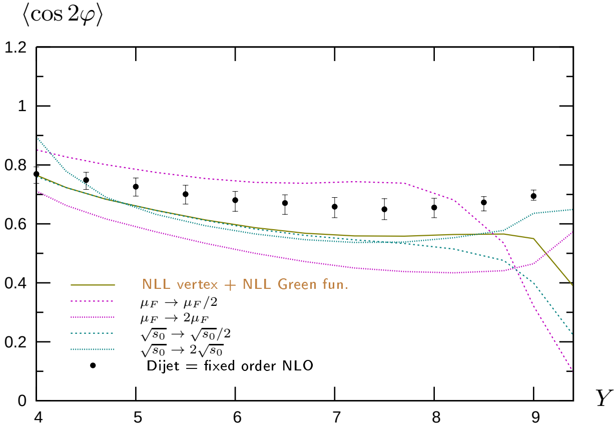

for typical CMS bins:

$35\,\mathrm{GeV} < |\mathbf{k}_{J,1}| < 60\,\mathrm{GeV}$

$50\,\mathrm{GeV} < |\mathbf{k}_{J,2}| < 60\,\mathrm{GeV}$

$0 < Y_1 < 4.7$

$0 < Y_2 < 4.7$

- Putting (almost) the same scale, exactly the same cuts, we get a difference between fixed order NLO and NLL BFKL for $4.5 < Y < 8.5$
- This difference is washed-out because of s_0 and μ dependency: $\langle \cos 2\varphi \rangle_{\mathrm{NLO}} \sim \langle \cos 2\varphi \rangle_{\mathrm{NLL\,BFKL}}$

Results: asymmetric config. $(|\mathbf{k}_{J,1\ \min}| = 35\,\mathrm{GeV}\,, |\mathbf{k}_{J,2\ \min}| = 50\,\mathrm{GeV})$ $\sqrt{s} = 7$ TeV

Azimuthal correlation $\langle\cos 2\varphi\rangle/\langle\cos\varphi\rangle$: fixed order NLO versus BFKL

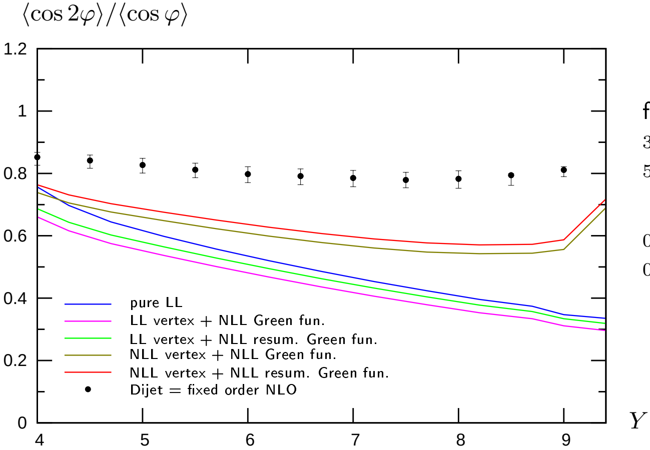

for typical CMS bins:

$35\,\mathrm{GeV} < |\mathbf{k}_{J,1}| < 60\,\mathrm{GeV}$

$50\,\mathrm{GeV} < |\mathbf{k}_{J,2}| < 60\,\mathrm{GeV}$

$0 < Y_1 < 4.7$

$0 < Y_2 < 4.7$

dots = based on the fixed order NLO parton generator *Dijet* (thanks to M. Fontannaz)

Results: asymmetric config. ($|\mathbf{k}_{J,1\,\min}| = 35\,\mathrm{GeV}$, $|\mathbf{k}_{J,2\,\min}| = 50\,\mathrm{GeV}$) $\sqrt{s} = 7$ TeV

Azimuthal correlation $\langle\cos 2\varphi\rangle/\langle\cos\varphi\rangle$: fixed order NLO versus NLL BFKL

Including uncertainties

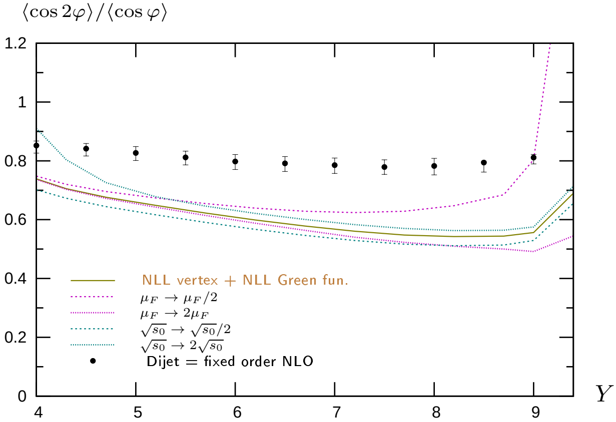

for typical CMS bins:

$35\,\mathrm{GeV} < |\mathbf{k}_{J,1}| < 60\,\mathrm{GeV}$

$50\,\mathrm{GeV} < |\mathbf{k}_{J,2}| < 60\,\mathrm{GeV}$

$0 < Y_1 < 4.7$

$0 < Y_2 < 4.7$

- fixed order NLO and NLL BFKL differ for $4.5 < Y < 8$

$$\frac{\langle\cos 2\varphi\rangle_{\mathrm{NLO}}}{\langle\cos\varphi\rangle_{\mathrm{NLO}}} > \frac{\langle\cos 2\varphi\rangle_{\mathrm{NLL\,BFKL}}}{\langle\cos\varphi\rangle_{\mathrm{NLL\,BFKL}}}$$

- This result is rather stable w.r.t s_0 and μ choices.

Results: asymmetric config. $(|\mathbf{k}_{J,1\ \min}| = 35\,\text{GeV}\,, |\mathbf{k}_{J,2\ \min}| = 50\,\text{GeV})$ $\sqrt{s} = 7$ TeV

Azimuthal correlation $\langle \cos 3\varphi \rangle / \langle \cos 2\varphi \rangle$: fixed order NLO versus BFKL

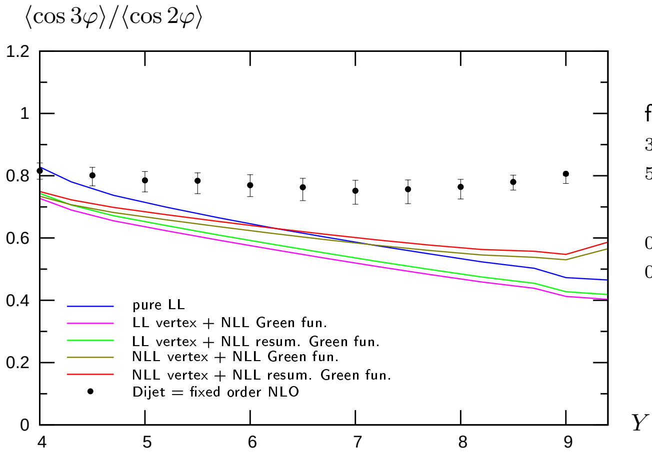

for typical CMS bins:

$35\,\text{GeV} < |\mathbf{k}_{J,1}| < 60\,\text{GeV}$

$50\,\text{GeV} < |\mathbf{k}_{J,2}| < 60\,\text{GeV}$

$0 < Y_1 < 4.7$

$0 < Y_2 < 4.7$

dots = based on the fixed order NLO parton generator *Dijet* (thanks to M. Fontannaz)

Results: asymmetric config. $(|\mathbf{k}_{J,1\,\min}| = 35\,\text{GeV}\,, |\mathbf{k}_{J,2\,\min}| = 50\,\text{GeV})$ $\sqrt{s} = 7$ TeV

Azimuthal correlation $\langle \cos 3\varphi \rangle / \langle \cos 2\varphi \rangle$: fixed order NLO versus BFKL

Including uncertainties

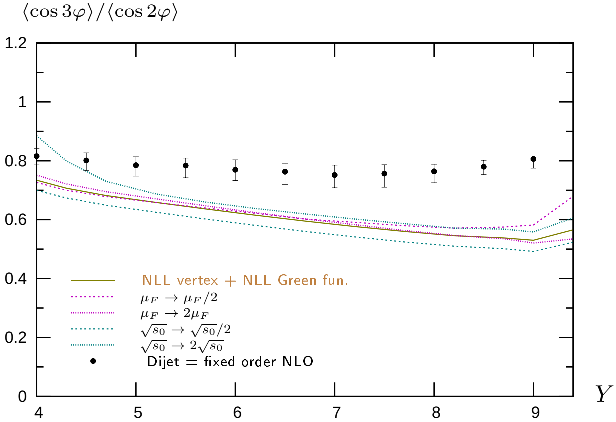

for typical CMS bins:

$35\,\text{GeV} < |\mathbf{k}_{J,1}| < 60\,\text{GeV}$

$50\,\text{GeV} < |\mathbf{k}_{J,2}| < 60\,\text{GeV}$

$0 < Y_1 < 4.7$

$0 < Y_2 < 4.7$

- fixed order NLO and NLL BFKL differ for $5.5 < Y < 8$

$$\frac{\langle \cos 3\varphi \rangle_{\text{NLO}}}{\langle \cos 2\varphi \rangle_{\text{NLO}}} > \frac{\langle \cos 3\varphi \rangle_{\text{NLL BFKL}}}{\langle \cos 2\varphi \rangle_{\text{NLL BFKL}}}$$

- This result is rather stable w.r.t s_0 and μ choices.

Conclusion

- We have deepen our complete NLL analysis of Mueller-Navelet jets
- The effect of NLL jets corrections is dramatic, similar to the NLL Green function corrections
- For the cross-section:
  - makes prediction much more stable with respect to variation of parameters (factorization scale, scale s_0 entering the rapidity definition, PDFs)
  - sizeably below fixed order NLO
- Surprisingly small decorrelation effect:
  - very close to fixed order NLO for $\langle \cos \varphi \rangle$ and $\langle \cos 2\varphi \rangle$
  - very flat in rapidity Y
  - still rather dependent on these parameters
- Collinear improved NLL BFKL and pure NLL leads to very similar result when summing over n
- The φ distr. is very strongly peaked around 0 and stable w.r.t. Y
- For $\langle \cos 2\varphi \rangle / \langle \cos \varphi \rangle$ and $\langle \cos 3\varphi \rangle / \langle \cos 2\varphi \rangle$ the differences between NLL BFKL and fixed order NLO are sizable, and stable w.r.t. to scale choices
- The predictions for these ratios are consistent with the recent CMS data
- VERY FRESH NEWS: an unnatural scale like $\mu_R = \mu_F = 8\sqrt{|\mathbf{k}_{J,1}|\,|\mathbf{k}_{J,2}|}$ provides a rather good description for all $\langle \cos \varphi \rangle$, $\langle \cos 2\varphi \rangle$, $\langle \cos 3\varphi \rangle$, all ratios $\langle \cos 2\varphi \rangle / \langle \cos \varphi \rangle$, $\langle \cos 3\varphi \rangle / \langle \cos 2\varphi \rangle$ and for the azimuthal distribution $\frac{1}{\sigma}\frac{d\sigma}{d\varphi}$ for $5 \lesssim Y \lesssim 8$ [BACKUP]

Results with an "unnatural" scale μ_F

Our prediction at NLL BFKL versus CMS data: $\langle \cos n\varphi \rangle$

$\langle \cos \varphi \rangle$

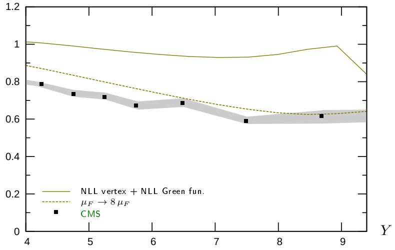

$\langle \cos 2\varphi \rangle$

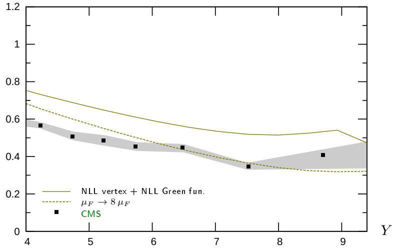

$\langle \cos 3\varphi \rangle$

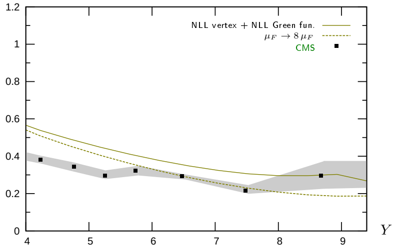

Results with an "unnatural" scale μ_F

Our prediction at NLL BFKL versus CMS data:
$\langle\cos 2\varphi\rangle/\langle\cos\varphi\rangle$ and $\langle\cos 3\varphi\rangle/\langle\cos 2\varphi\rangle$

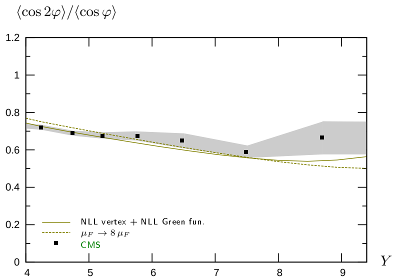

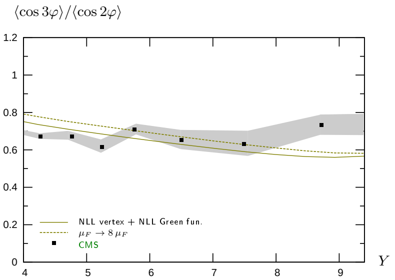

Results with an "unnatural" scale μ_F

Our prediction at NLL BFKL versus CMS data: $\frac{1}{\sigma}\frac{d\sigma}{d\varphi}$

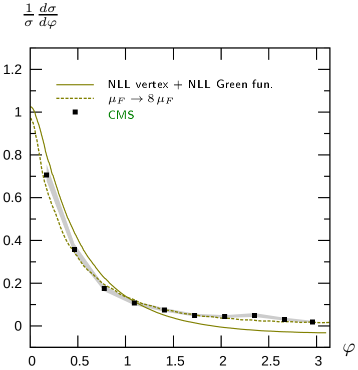

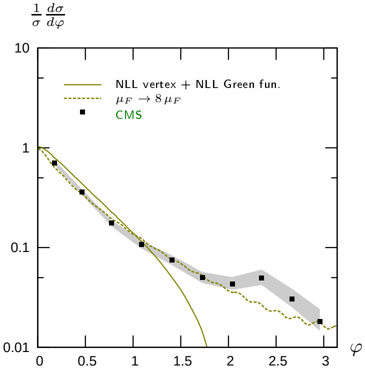

Here $Y = Y_1 + Y_2$ is integrated over the range $[6, 9.4]$ with $0 < Y_i < 4.7$.

Can Mueller-Navelet jets be a manifestation of multiparton interactions?

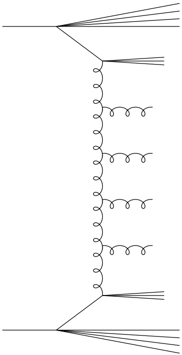

MN jets in the single partonic model

+

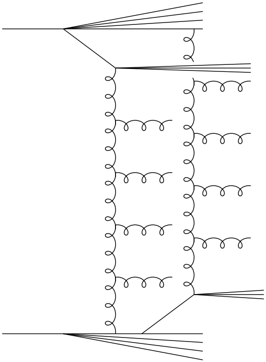

MN jets in MPI

Can Mueller-Navelet jets be a manifestation of multiparton interactions?

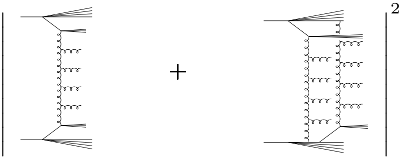

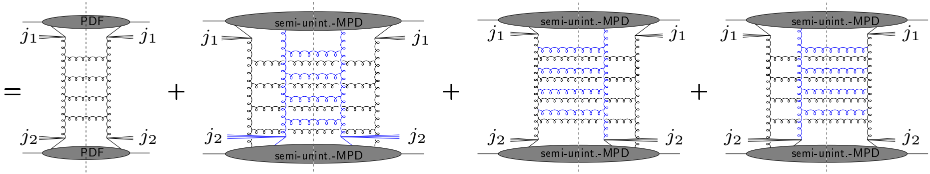

single $\mathbb{P}$ ladder | two $\mathbb{P}$ ladders | interferences

scaling: $s^{\alpha_{\mathbb{P}}}$ | (??) $s^{2\alpha_{\mathbb{P}}}$ | ??

- The twist counting is not easy for MPI kinds of contributions at small x
- $k_{\perp 1,2}$ are not integrated $\Rightarrow$ MPI may be competitive, and enhanced by small-x resummation
- Interference terms are not governed by BJKP (this is not a fully interacting 3-reggeons system) (for BJKP, $\alpha_{\mathbb{P}} < 1 \Rightarrow$ suppressed)

Jet vertex: LL versus NLL

$\mathbf{k}, \mathbf{k}' =$ Euclidian two dimensional vectors

LL jet vertex:

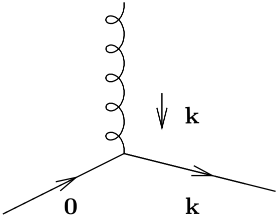

NLL jet vertex:

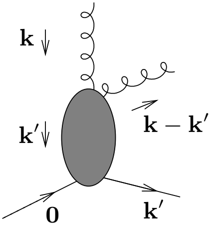

Jet vertex: jet algorithms

Jet algorithms

- a jet algorithm should be IR safe, both for soft and collinear singularities
- the most common jet algorithm are:
  - k_t algorithms (IR safe but time consuming for multiple jets configurations)
  - cone algorithm (not IR safe in general; can be made IR safe at NLO: Ellis, Kunszt, Soper)

Jet vertex: jet algorithms

Cone jet algorithm at NLO (Ellis, Kunszt, Soper)

- Should partons $(|\mathbf{p}_1|, \phi_1, y_1)$ and $(\mathbf{p}_2|, \phi_2, y_2)$ combined in a single jet? $|\mathbf{p}_i|$ =transverse energy deposit in the calorimeter cell i of parameter $\Omega = (y_i, \phi_i)$ in $y - \phi$ plane
- define transverse energy of the jet: $p_J = |\mathbf{p}_1| + |\mathbf{p}_2|$
- jet axis:

$$\Omega_c \begin{cases} y_J = \dfrac{|\mathbf{p}_1|\, y_1 + |\mathbf{p}_2|\, y_2}{p_J} \\[2ex] \phi_J = \dfrac{|\mathbf{p}_1|\, \phi_1 + |\mathbf{p}_2|\, \phi_2}{p_J} \end{cases}$$

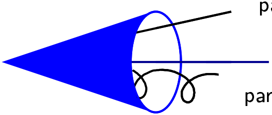

$\Omega = (y_i, \phi_i)$ in $y - \phi$ plane

If distances $|\Omega_i - \Omega_c|^2 \equiv (y_i - y_c)^2 + (\phi_i - \phi_c)^2 < R^2$ $(i = 1$ and $i = 2)$

$\Longrightarrow$ partons 1 and 2 are in the same cone Ω_c

combined condition: $|\Omega_1 - \Omega_2| < \dfrac{|\mathbf{p}_1| + |\mathbf{p}_2|}{max(|\mathbf{p}_1|, |\mathbf{p}_2|)} R$

Jet vertex: LL versus NLL and jet algorithms

LL jet vertex and cone algorithm

$\mathbf{k}, \mathbf{k}'$ = Euclidian two dimensional vectors

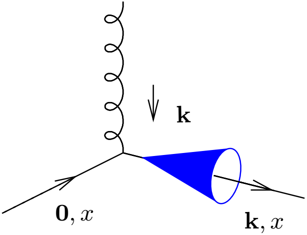

$$\mathcal{S}_J^{(2)}(k_\perp; x) = \delta\left(1 - \frac{x_J}{x}\right) |\mathbf{k}|\, \delta^{(2)}(\mathbf{k} - \mathbf{k}_J)$$

Jet vertex: LL versus NLL and jet algorithms

NLL jet vertex and cone algorithm

$\mathbf{k}, \mathbf{k}'$ = Euclidian two dimensional vectors

$$\mathcal{S}_J^{(3,\text{cone})}(\mathbf{k}', \mathbf{k}-\mathbf{k}', xz; x) =$$

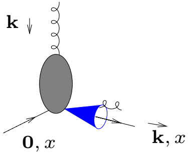

$$\mathcal{S}_J^{(2)}(\mathbf{k}, x)\, \Theta\left(\left[\frac{|\mathbf{k}-\mathbf{k}'|+|\mathbf{k}'|}{\max(|\mathbf{k}-\mathbf{k}'|,|\mathbf{k}'|)} R_{\text{cone}}\right]^2 - \left[\Delta y^2 + \Delta\phi^2\right]\right)$$

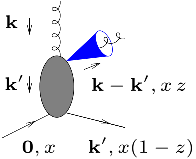

$$+\, \mathcal{S}_J^{(2)}(\mathbf{k}-\mathbf{k}', xz)\, \Theta\left(\left[\Delta y^2 + \Delta\phi^2\right] - \left[\frac{|\mathbf{k}-\mathbf{k}'|+|\mathbf{k}'|}{\max(|\mathbf{k}-\mathbf{k}'|,|\mathbf{k}'|)} R_{\text{cone}}\right]^2\right)$$

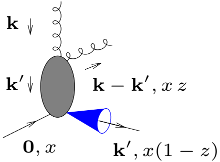

$$+\, \mathcal{S}_J^{(2)}(\mathbf{k}', x(1-z))\, \Theta\left(\left[\Delta y^2 + \Delta\phi^2\right] - \left[\frac{|\mathbf{k}-\mathbf{k}'|+|\mathbf{k}'|}{\max(|\mathbf{k}-\mathbf{k}'|,|\mathbf{k}'|)} R_{\text{cone}}\right]^2\right),$$

Mueller-Navelet jets at NLL and finiteness

Using a IR safe jet algorithm, Mueller-Navelet jets at NLL are finite

- UV sector:
  - the NLL impact factor contains UV divergencies $1/\epsilon$
  - they are absorbed by the renormalization of the coupling: $\alpha_S \longrightarrow \alpha_S(\mu_R)$
- IR sector:
  - PDF have IR collinear singularities: pole $1/\epsilon$ at LO
  - these collinear singularities can be compensated by collinear singularities of the two jets vertices and the real part of the BFKL kernel
  - the remaining collinear singularities compensate exactly among themselves
  - soft singularities of the real and virtual BFKL kernel, and of the jets vertices compensates among themselves

This was shown for both quark and gluon initiated vertices (Bartels, Colferai, Vacca)

BFKL Green's function at NLL

NLL Green's function: rely on LL BFKL eigenfunctions

- NLL BFKLkernel is not conformal invariant
- LL $E_{n,\nu}$ are not anymore eigenfunction
- this can be overcome by considering the eigenvalue as an operator with a part containing $\frac{\partial}{\partial \nu}$
- it acts on the impact factor

$$\omega(n,\nu) = \bar{\alpha}_s \chi_0 \left(|n|, \frac{1}{2} + i\nu\right) + \bar{\alpha}_s^2 \left[\chi_1 \left(|n|, \frac{1}{2} + i\nu\right)\right.$$

$$\left. - \frac{\pi b_0}{2N_c} \chi_0 \left(|n|, \frac{1}{2} + i\nu\right) \underbrace{\left\{-2 \ln \mu_R^2 - i \frac{\partial}{\partial \nu} \ln \frac{C_{n,\nu}(|\mathbf{k}_{J,1}|, x_{J,1})}{C_{n,\nu}(|\mathbf{k}_{J,2}|, x_{J,2})}\right\}}_{2 \ln \frac{|\mathbf{k}_{J,1}| \cdot |\mathbf{k}_{J,2}|}{\mu_R^2}} \right],$$

LL substraction and s_0

- one sums up $\sum(\alpha_s \ln \hat{s}/s_0)^n + \alpha_s \sum(\alpha_s \ln \hat{s}/s_0)^n \quad (\hat{s} = x_1\, x_2\, s)$
- at LL s_0 is arbitrary
- natural choice: $s_0 = \sqrt{s_{0,1}\, s_{0,2}}$ $\quad s_{0,i}$ for each of the scattering objects
  - possible choice: $s_{0,i} = (|\mathbf{k}_J| + |\mathbf{k}_J - \mathbf{k}|)^2$ (Bartels, Colferai, Vacca)
    - but depend on $\mathbf{k}$, which is integrated over
    - $\hat{s}$ is not an external scale ($x_{1,2}$ are integrated over)
  - we prefer

$$\left.\begin{aligned} s_{0,1} &= (|\mathbf{k}_{J,1}| + |\mathbf{k}_{J,1} - \mathbf{k}_1|)^2 \;\to\; s'_{0,1} = \frac{x_1^2}{x_{J,1}^2}\mathbf{k}_{J,1}^2 \\ s_{0,2} &= (|\mathbf{k}_{J,2}| + |\mathbf{k}_{J,2} - \mathbf{k}_2|)^2 \;\to\; s'_{0,2} = \frac{x_2^2}{x_{J,2}^2}\mathbf{k}_{J,2}^2 \end{aligned}\right\} \quad \frac{\hat{s}}{s_0} \;\to\; \frac{\hat{s}}{s'_0} = \frac{x_{J,1}\, x_{J_2}\, s}{|\mathbf{k}_{J,1}|\,|\mathbf{k}_{J,2}|} = e^{y_{J,1}-y_{J,2}} \equiv e^Y$$

- $s_0 \to s'_0$ affects
  - the BFKL NLL Green function
  - the impact factors:

$$\Phi_{\rm NLL}(\mathbf{k}_i; s'_{0,i}) = \Phi_{\rm NLL}(\mathbf{k}_i; s_{0,i}) + \int \mathrm{d}^2\mathbf{k}'\, \Phi_{\rm LL}(\mathbf{k}'_i)\, \mathcal{K}_{\rm LL}(\mathbf{k}'_i, \mathbf{k}_i) \frac{1}{2} \ln \frac{s'_{0,i}}{s_{0,i}} \qquad (1)$$

- numerical stabilities (non azimuthal averaging of LL substraction) improved with the choice $s_{0,i} = (\mathbf{k}_i - 2\mathbf{k}_{J,i})^2$
  (then replaced by $s'_{0,i}$ after numerical integration)
- (1) can be used to test $s_0 \to \lambda\, s_0$ dependence

Collinear improvement at NLL

Collinear improved Green's function at NLL

- one may improve the NLL BFKL kernel for $n = 0$ by imposing its compatibility with DGLAP in the collinear limit
  Salam; Ciafaloni, Colferai
- usual (anti)collinear poles in $\gamma = 1/2 + i\nu$ (resp. $1-\gamma$) are shifted by $\omega/2$
- one practical implementation:
  - the new kernel $\bar{\alpha}_s \chi^{(1)}(\gamma,\omega)$ with shifted poles replaces

    $\bar{\alpha}_s \chi_0(\gamma,0) + \bar{\alpha}_s^2 \chi_1(\gamma,0)$
  - $\omega(0,\nu)$ is obtained by solving the implicit equation

    $$\omega(0,\nu) = \bar{\alpha}_s \chi^{(1)}(\gamma,\omega(0,\nu))$$

    for $\omega(n,\nu)$ numerically.
- there is no need for any jet vertex improvement because of the absence of γ and $1-\gamma$ poles (numerical proof using Cauchy theorem "backward")
- this can be extended for all n

Motivation for asymmetric configurations

- Initial state radiation (unseen) produces divergencies if one touches the collinear singularity $\mathbf{q}^2 \to 0$

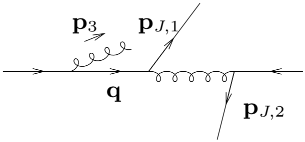

- they are compensated by virtual corrections
- this compensation is in practice difficult to implement when for some reason this additional emission is in a "corner" of the phase space (dip in the differential cross-section)
- this is the case when $\mathbf{p}_1 + \mathbf{p}_2 \to 0$
- this calls for a resummation of large remaing logs $\Rightarrow$ Sudakov resummation

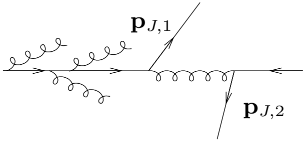

Motivation for asymmetric configurations

- since these resummation have never been investigated in this context, one should better avoid that region
- note that for BFKL, due to additional emission between the two jets, one may expect a less severe problem (at least a smearing in the dip region $|\mathbf{p}_1| \sim |\mathbf{p}_2|$)

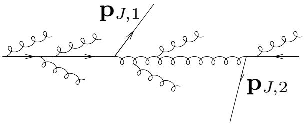

- this may however not mean that the region $|\mathbf{p}_1| \sim |\mathbf{p}_2|$ is perfectly trustable even in a BFKL type of treatment
- we now investigate a region where NLL DGLAP is under control